
IMPLEMENTATION STUDY OF COST-EFFECTIVE VERIFICATION FOR PIETRZAK’S VDF IN ETHEREUM SMART CONTRACTS

A PREPRINT

Suhyeon Lee [§]
Tokamak Network
suhyeon@tokamak.network

Euisin Gee [§]
School of Cybersecurity
Korea University
usgee@korea.ac.kr
Onther
justin.g@onther.io

Junghee Lee
School of Cybersecurity
Korea University
j_lee@korea.ac.kr

August 19, 2024

ABSTRACT

Verifiable Delay Function (VDF) is a cryptographic concept that ensures a minimum delay before output through sequential processing, which is resistant to parallel computing. One of the significant VDF protocols academically reviewed is the VDF protocol proposed by Pietrzak. However, for the blockchain environment, the Pietrzak VDF has drawbacks including long proof size and recursive protocol computation. In this paper, we present an implementation study of Pietrzak VDF verification on Ethereum Virtual Machine (EVM). We found that the discussion in the Pietrzak’s original paper can help a clear optimization in EVM where the costs of computation are predefined as the specific amounts of gas. In our results, the cost of VDF verification can be reduced from 4M to 2M gas, and the proof length can be generated under 8 KB with the 2048-bit RSA key length, which is much smaller than the previous expectation.

Keywords Ethereum · blockchain security · cryptographic protocol · decentralized application · gas optimization · verifiable delay function

1 Introduction

The Verifiable Delay Function (VDF)’s major role is to guarantee a specific delay for evaluation. It can play an important role in security applications. The most notable application of blockchain using VDF is a distributed randomness beacon. VDFs do not directly generate a random number. Rather, they help to guarantee the liveness of a random number generation scheme, Commit-Reveal, by recovering a random number when the reveal phase fails. This has led Ethereum, one of the largest cryptocurrencies, to include VDFs in their future roadmap for the RANDAO block proposer selection mechanism.

In recent years, several VDF mechanisms have been proposed [1–4]; however, the concept of VDFs remains relatively new. This indicates that we need comprehensive research on VDFs across various dimensions. For example, recently found parallel computation mechanisms for VDF evaluation [5, 6] show that we need more research on the squaring computation. On the other hand, there is a scarcity of implementation research [7] on VDFs. In this paper, we focus on VDF implementation on EVM, one of the leading blockchain environments.

Our goal is to efficiently implement VDF verification within smart contracts, providing a foundation for EVM security applications utilizing VDFs. Specifically, we focus on the Pietrzak VDF [2] for two key reasons: First, the Wesolowski VDF [1], another major VDF, requires a hash-to-prime function, which is challenging to implement directly in smart contracts. Second, we hypothesize that the performance optimization technique discussed by Pietrzak [2] could significantly reduce the overall cost within the EVM environment. As a result of this focus, our research

[§]These authors contributed equally to this work.

demonstrates through theoretical analysis and experiments that Pietrzak VDF verification can be effectively utilized within EVM-compatible smart contracts.

The contributions of this paper are as follows:

- To the best of our knowledge, this research presents the first academic study of Pietrzak VDF implementation on smart contracts.
- Through theoretical analysis, we demonstrated the existence of a unique parameter that reduces the proof length. Additionally, the actual implementation results were consistent with our theoretical expectations.
- Contrary to previous studies' expectations, we demonstrated that the Pietrzak VDF could be utilized in the Ethereum environment with under 8 KB calldata size with the 2048-bit RSA key length.

The rest of the paper is organized as follows: Section 2 reviews related works on VDFs. Section 3 describes the target algorithm and experiment environment. In Section 4, we measure the gas costs for VDF verification on the EVM and formulate them into a function using regression. Section 5 analyzes the optimal parameters for VDF verification costs and presents experimental results that demonstrate the theoretical analysis. Finally, Section 6 concludes the paper with a discussion of further research directions. The source code for our implementation is available in the Appendix A.

2 Related Works

The concept of recursive computation for delayed output was firstly proposed as the "Time-Lock Puzzle" by Rivest et al. [8]. The Time-Lock Puzzle does not include efficient public verifiability of the solution. This was later addressed by Mahmoody et al. in their Proof of Sequential Work (PoSW) [9]. Lenstra and Wesolowski proposed Sloth, which is considered the first Verifiable Delay Function (VDF) style mechanism [3]. Boneh et al. [10] formalized the concept of VDF. Following the introduction of VDFs, various mechanisms were proposed, among which the VDFs by Wesolowski [1] and Pietrzak [2] had unique advantages in terms of efficiency and security. For the use in blockchain, Veedo and Minroot [4] were proposed for Starknet and RANDAO respectively. However, recent findings by Biryukov et al. [5] and Leurent [6] demonstrate that distributed algorithms for modular squaring exist. This implies that the fundamental assumption of using sequential squaring puzzles is not valid, highlighting the need for further research on this issue.

Not only theoretical research, but also implementation studies are crucial for approaching practical applications. However, such studies appear to have been conducted in a rather limited scope. A significant contribution is the study by Attias et al. [7], which provides a comprehensive implementation analysis of two leading VDFs, Pietrzak and Wesolowski. Their work meticulously evaluates the performance of VDFs' evaluation, proof generation, and verification. Their work provided us with insight into the research and optimization techniques for VDFs. However, they expected the Pietrzak VDF would not be viable for blockchains. This is contrary to our results that presented the feasibility of the Pietrzak VDF on Ethereum smart contracts. Choi et al. [11] proposed three practical commit-reveal-recover protocols. They incorporated the Wesolowski VDF into Ethereum smart contracts for the purpose of demonstration. Our research covers VDF verification, which corresponds to the Proof-of-Exponentiation (PoE) stated in their work.

3 Implementation Target and Environment

In this section, we provide the target algorithm and environment. Firstly, we define the Pietrzak VDF verification algorithm we aim to implement. Secondly, we describe the experiment environment for the cost measurement.

3.1 Pietrzak VDF verification

Algorithm 1 outlines the Pietrzak VDF verification process. Given that a prover insists the VDF evaluation $x^{2^T} = y$ with the time delay parameter $T = 2^\tau$, the set of halving proof $\{\pi_i\}_{i=1}^\tau$, and the modulus N . It repeats the halving protocol (lines 5 – 13) until the verifier can simply check the result by squaring the base. The halving protocol reduces the number of exponentiations required for verification by half. The halving protocol outputs x_1, y_1 and the proof π reasoning $x_1^{2^{2^\tau-1}} = y_1$. Therefore, the verifier essentially needs to repeat the halving protocol τ times for the minimal exponentiation.

One drawback of the Pietrzak VDF is that as the time delay parameter increases, the proof size and the number of halving protocol repetitions for the verifier also increase. In the original paper proposing the Pietrzak VDF, a method to enhance efficiency was suggested. Since the halving protocol also consumes resources, the verifier can repeat the

halving protocol $\tau - \delta$ times instead of τ times. Then, the verifier needs to check $x^{2^{2^\delta}} \stackrel{?}{=} y$. Furthermore, this approach helps to reduce the size of the proof. Algorithm 2 describes this refined verification procedure.

In most systems, the costs of each computation and the overhead due to proof size are dependent on the specific system environment, making it difficult to determine the optimal value for the proof shortening parameter, δ . However, in the EVM, the costs for data (calldata) and arithmetic computations are predefined. This led us to hypothesize that it is possible to identify the optimal δ value for implementation, thereby minimizing both computation and calldata costs in blockchain environments.

Algorithm 1 Pietrzak VDF Verification

```

1: input:  $x, y, T, \{\pi_i\}_{i=1}^\tau, N$ 
2: output: True or False
3:  $\tau \leftarrow \lfloor \log_2(T) \rfloor$ 
4:  $(x_1, y_1) \leftarrow (x, y)$ 
5: for  $i \leftarrow 1$  to  $\tau$  do
6:    $v_i \leftarrow \pi_i$ 
7:    $r_i \leftarrow \text{keccak256}(x_i || y_i || v_i)$ 
8:    $x_{i+1} \leftarrow x_i^{r_i} \cdot v_i \bmod N$ 
9:   if  $T/2^{i-1}$  is odd then
10:     $y_i \leftarrow y_i^2 \bmod N$ 
11:   end if
12:    $y_{i+1} \leftarrow v_i^{r_i} \cdot y_i \bmod N$ 
13: end for
14: if  $y_{\tau+1} = x_{\tau+1}^2$  then
15:   return True
16: else
17:   return False
18: end if
```

Algorithm 2 Refined Pietrzak VDF Verification

```

1: input:  $x, y, T, \delta, \{\pi_i\}_{i=1}^{\tau-\delta}, N$ 
2: output: True or False
3:  $\tau \leftarrow \lfloor \log_2(T) \rfloor$ 
4:  $(x_1, y_1) \leftarrow (x, y)$ 
5: for  $i \leftarrow 1$  to  $\tau - \delta$  do
6:    $v_i \leftarrow \pi_i$ 
7:    $r_i \leftarrow \text{keccak256}(x_i || y_i || v_i)$ 
8:    $x_{i+1} \leftarrow x_i^{r_i} \cdot v_i \bmod N$ 
9:   if  $T/2^{i-1}$  is odd then
10:     $y_i \leftarrow y_i^2 \bmod N$ 
11:   end if
12:    $y_{i+1} \leftarrow v_i^{r_i} \cdot y_i \bmod N$ 
13: end for
14: if  $y_{\tau-\delta+1} = x_{\tau-\delta+1}^{2^{2^\delta}}$  then
15:   return True
16: else
17:   return False
18: end if
```

3.2 Target Bit Length and Target Delay

The security of Pietrzak VDF configuration depends on the difficulty of the prime factoring problem, akin to that in the RSA encryption system. Currently, a 2048-bit key length is deemed sufficient for maintaining security standards. However, considering potential advancements in computational capabilities, a 3072-bit key length might be necessary after ten years. Therefore, our experiments included tests with both 2048-bit and 3072-bit settings for VDFs.

In a recent study on VDF implementation using C++ [7], VDF evaluation times with the time delay parameter T ranging from 2^{20} to 2^{25} can be completed within one minute with a personal CPU. The evaluation involves performing $y = x^{2^T}$. In other words, the target range for τ is 20 – 25 where $T = 2^\tau$. We chose to conduct our VDF experiments within the same parameter range, as it strikes a balance between computational feasibility and practical utility while avoiding excessive resource consumption.

3.3 Environment for Gas Usage Measurement

3.3.1 Development Environment and Tools

The development of the contract was conducted using Solidity version 0.8.26 and EVM version Cancun. At the start of the development process, it was the latest compiler version fully supported by Foundry, which is a comprehensive Ethereum development toolchain that provides a robust environment for building, testing, and debugging smart contracts. Furthermore, gas optimization is best achieved with the latest version of the compiler.

3.3.2 Optimizer Configuration

The core parameter for the Solidity optimizer configuration is `Runs` which indicates how often each opcode will be used in the deployed contract. That is, higher `Runs` implies less gas cost for execution and higher gas cost for deployment. We set the optimizer parameter `Runs` to 4,294,967,295($2^{32} - 1$), which is the maximum value of the parameter, indicating the highest level of optimization for execution.

We set up Via-IR (Intermediate Representation) and the Yul optimizer in the Solidity compiler to generate efficient bytecode. Via-IR helps efficiency, security, and simplicity in code generation by deviating from the direct compilation of Solidity code to EVM bytecode. Instead, via-IR processes an intermediate step where Yul code, an intermediate representation, is generated.

In this step, we could enhance the Yul optimizer’s efficiency by replacing the `msize()` operation with the free memory pointer. This adjustment necessitated manual updates to the memory indexes, a process rigorously tested to ensure the integrity of our implementation. We also applied memory-safe assembly blocks in our code. This change not only aligns with Solidity’s memory model but also activates Via-IR in the compiler settings, resulting in significant gas savings.

3.3.3 Gas Measurement in Local Testing Environment

As the test target code, we implemented contracts for each test in one main source file ensuring that each contract contains only one external function. This approach minimizes the error margin that can arise when multiple external functions are present, as the order of the function selectors impacts the `gasUsed`.

For the cost (gas usage) measurement, we utilized the Anvil node, provided by the Foundry toolchain, to create a local testing environment. The gas usage was obtained using the Forge testing framework provided by Foundry. The Forge standard library’s `Test` contract includes the `lastCallGas()` function, which retrieves the `gasUsed` in the last call. Additionally, `isolate` flag must be set when running the Forge’s test command to ensure all top-level calls are executed as separate transactions in distinct EVM contexts. This setup allows for more precise gas accounting. It is important to note that the actual gas cost incurred on the real network is determined by multiplying the estimated `gasUsed` by the `gasPrice` at the Ethereum network circumstance.

4 Cost measurement and approximation

In this section, we introduce the data structure we used to send VDF proofs in the Ethereum transaction calldata. Then, we investigate the gas cost to send VDF proofs and regress the results to linear functions for the next sections.

4.1 Data Structure

In this study, the VDFs are implemented with key sizes of 2048 and 3072 bits. However, the EVM natively supports arithmetic operators only up to 256-bit numbers. To facilitate efficient computation of numbers exceeding 256 bits, it is necessary to employ customized data formats. We revised the big number library implementation for Solidity developed by Firo [12]. The original data structure in this library includes bytes data (`bytes val`), bit length (`uint bitlen`), and a sign indicator (`bool neg`). Among the three elements, we deleted the sign indicator and its related low-level logic since our implementation does not require handling negative values. This library optimizes on-chain operations such as addition and subtraction by adding leading zeros for 32-byte alignment with the EVM’s memory word size, eliminating offset management. Also, it utilizes the bit length data field to optimize multiplication and comparison operations. Therefore, we format the bytes data and pre-calculate bit length off-chain before submission, significantly reducing unnecessary on-chain computations. For example, the data format for a 2048-bit representation in JSON is as shown in Listing 1. In this way, we can reduce the gas cost even though the calldata size increases. This decision is reasonable because the primary goal is to reduce the gas cost, not the transaction calldata size.

Listing 1 Calldata for a Big Number Example

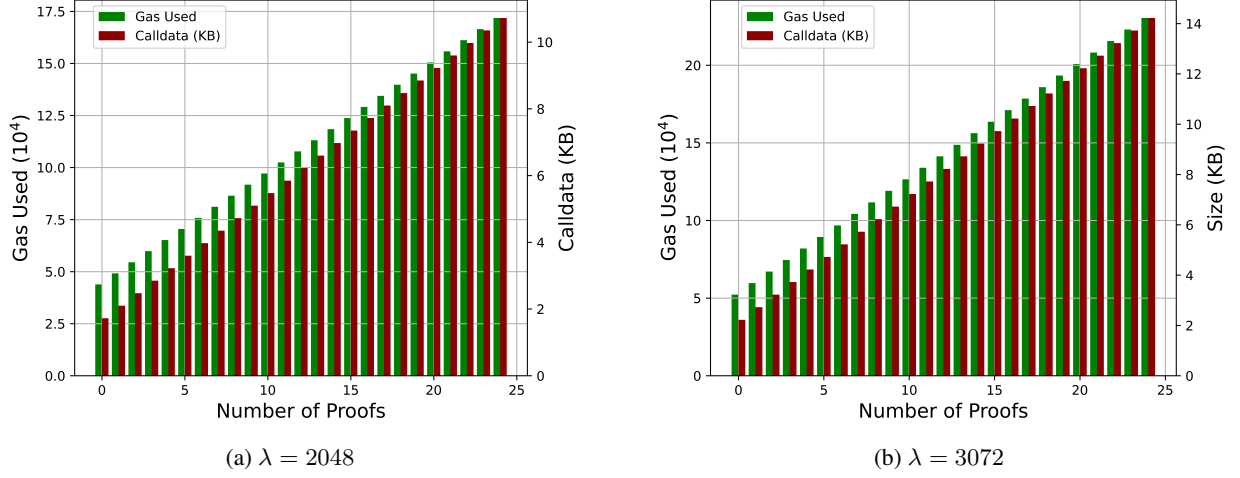
```

1 {
2   "big_number": {
3     "val": "0x4621c26320fe0924bba1b7d5bc863495b9f0db3823b12a9a18e21
           d23.....b2127fd6390f5f6234a164bd39d1dd6884b768c4dd790586ee",
4     "bitlen": 2047
5   }
6 }
```

4.2 Gas Cost for Calldata and Dispatch

The gas cost for Ethereum transaction calldata, as described in EIP-2028 "Transaction data gas cost reduction" [13], is divided into two cases: 16 gas per non-zero byte and 4 gas per zero byte.

Figure 1: Experiment results of the calldata and its dispatch cost



Considering the above gas pricing, we can calculate the cost for sending one 2048-bit length data in the aforementioned data structure. Taking into account the probability of each byte being non-zero, which is $\frac{1}{256}$, the expected gas cost for sending one 2048-bit length data is 1036 gas. The gas for the Big Number structure is added to this.

In our implementation, the function `verifyRecursiveHalvingProof` processes the refined verification, Algorithm 2. A call to this function involves encoding parameter values. The process starts by computing the `keccak256` of the UTF-8 byte representation of the string¹, then using the first four bytes, which results in `0xd8e6ac60`.

For static types such as `uint256`, fields including `delta` and `T` are padded to 32 bytes. On the other hand, In EVM, dynamic types, including `bytes`, `struct`, and dynamic arrays, are encoded by specifying an offset to the start of the data, its length, and then the data itself. This routine is applied recursively for nested dynamic types. In case of `BigNumber[] memory v`, it is the dynamic array of dynamic type `struct BigNumber` that contains dynamic bytes `val`. So the way dynamic types are encoded is recursively applied to each halving proof `v`.

Parameters such as T , δ , λ , and parameter count (e.g., 6 in our model) determine the offsets and lengths. The gas usage for data depends probabilistically on the distribution of zero and non-zero bytes in the data. Since EVM organizes memory in 32-byte words, we can consider the same number of word is repeated when data is repeated. Finally, we can predict the approximate gas usage of calldata using this EVM data construction structure.

Considering the prediction of data and its cost, we performed experiments to test the size of calldata and the related gas usage. The related gas usage comprises of the intrinsic gas and data dispatching gas. The intrinsic gas in EVM refers the minimum cost for a transaction. It contains the constant transaction cost (21000 gas) and the cost for data supply. For verification, we need not only to allocate data in a transaction, but also to dispatch data into the verification function. The dispatching cost is proportional to the data size. Therefore, we decided to include the dispatching cost into the data cost in this study. Figure 1a for $\lambda = 2048$ and 1b for $\lambda = 3072$ show the calldata size with the number of proofs and the related gas usage. We can see the gas usage and the calldata size simply and linearly increase with the number of proofs.

Finally, to describe the relationship between transaction size and gas costs, we performed a basic regression analysis. By applying the least squares method to approximate the best fit, we derive the following linear regression equations 1 and 2 for data sizes of 2048 and 3072 bytes, respectively:

$$\mathcal{G}_{data,2048}(\tau) = 5295.73 \cdot \tau + 37610.11 \quad (1)$$

$$\mathcal{G}_{data,3072}(\tau) = 7389.31 \cdot \tau + 43943.88 \quad (2)$$

These equations estimate the gas cost \mathcal{G} as a function of transaction size τ , highlighting the increase in required gas with larger transaction calldata.

¹`verifyRecursiveHalvingProof((bytes,uint256)[],(bytes,uint256),(bytes,uint256),(bytes,uint256),uint256,uint256)`

Figure 2: Experiment results of the halving algorithm cost

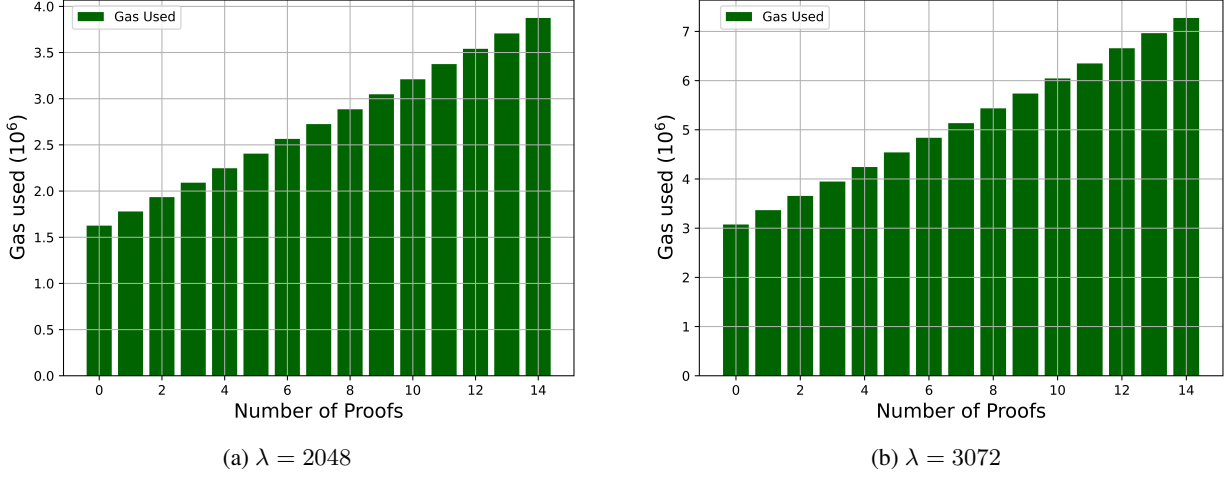
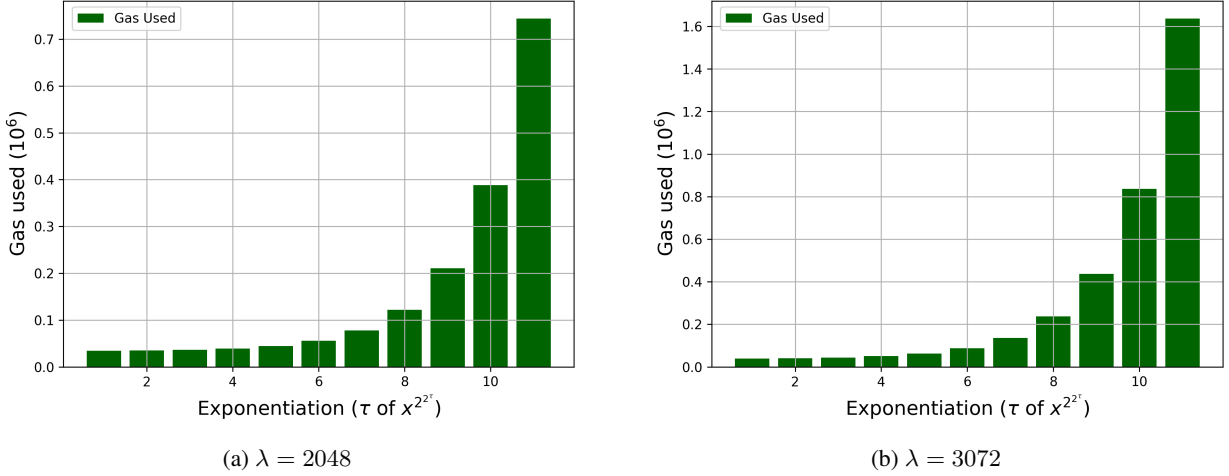


Figure 3: Experiment results of the ModExp cost



4.3 Modular Exponentiation Cost

EIP-198 [14], known for "Big Integer Modular Exponentiation", introduced the ModExp (Modular Exponential) precompiled contract to the EVM, offering a streamlined and cost-efficient approach for large integer modular exponentiation.² As it is obvious that a precompile provides the best efficiency, we applied ModExp for both the modular exponentiation and multi-exponentiation operations in the implementation in Algorithm 2. In Figure 3a and Figure 3b illustrating the experiment results, the pricing of ModExp is linearly proportional to the number of exponentiation as $\mathcal{G}(T) = aT + b$, where we denote τ as the logarithmic value of T . We could get the following results from a simple regression process.

$$\mathcal{G}_{exp,2048}(\tau) = 346.92 \cdot 2^\tau + 33432.08 \quad (3)$$

$$\mathcal{G}_{exp,3072}(\tau) = 780.83 \cdot 2^\tau + 37445.60 \quad (4)$$

²EIP-2565 [15] contributed to further refining the gas cost model for these modular exponentiation operations by proposing adjustments to the pricing formula.

4.4 Halving Cost

The halving cost of the arithmetic operations in the verification indicates the gas usage for lines 5 – 13 in Algorithm 2. The modular exponentiation operations in lines 8, 10, and 12 use the precompiled ModExp. For simplicity, as we assumed $T = 2^\tau$, in this case, the if statement in line 9 is always false, therefore line 10 is never executed. Hence, the gas usage is clearly proportional to the number of the repetition time, that is, $\tau - \delta$.

The results of our experiments demonstrate the anticipated correlation. Figure 2a and Figure 2b display the gas cost of the repeated halving operations with $\lambda = 2048$ and $\lambda = 3072$ correspondingly. The data exhibits a clear linear relationship, allowing us to perform a regression analysis and model the results using a linear function. By employing the method of least squares approximation, we obtain the subsequent functions as Equation 5 and 6:

$$\mathcal{G}_{\text{halving},2048}(\tau) = 160604.41 \cdot \tau - 157178.66 \quad (5)$$

$$\mathcal{G}_{\text{halving},3072}(x) = 299896.98 \cdot \tau - 248119.67 \quad (6)$$

5 Cost-Effective Implementation

This section explains the implementation of a cost-efficient Pietrzak VDF verifier as an Ethereum smart contract. In the beginning, we utilize the gas cost outcomes obtained from the preceding sections to make theoretical predictions for the optimized proof generating process. Secondly, we prove that there exists a unique δ that minimizes the gas usage for VDF verification, and this minimization is independent of τ . In the end, we compare the anticipated outcome based on theory with the actual results obtained from the experiment.

5.1 Theoretical Analysis on Proof Generation for Gas Usage Optimization

The optimized proof generation in this research means minimizing the verification gas cost in EVM. We can define the total gas cost function $\mathcal{G}_{\text{total}}$ using the previous regression results.

$$\mathcal{G}_{\text{total}}(\tau, \delta) = \mathcal{G}_{\text{calldata}} + \mathcal{G}_{\text{halving}} + \mathcal{G}_{\text{exp}} + C \quad (7)$$

$$= (\alpha \cdot (\tau - \delta) + c_1) + (\beta \cdot (\tau - \delta) + c_2) + (\gamma \cdot 2^\delta + c_3) + C \quad (8)$$

$$= (\alpha + \beta)(\tau - \delta) + \gamma \cdot 2^\delta + C' \quad (9)$$

Then, we get Theorem 1 says that there is a unique delta minimizing the total gas cost.

Theorem 1. *The function $\mathcal{G}_{\text{total}}(\tau, \delta)$ has exactly one unique minimum for δ when $\tau > \delta = \log_2(\alpha + \beta) - \log_2(\ln 2 \cdot \gamma)$.*

Proof. See Appendix B. □

Also, we denote the minimizing δ as

$$\delta_m = \arg \min_{\delta} \mathcal{G}_{\text{total}}(\tau, \delta). \quad (10)$$

From Theorem 1, we can get the unique δ_m optimizing the gas cost. Applying all the regression results in Equation 1, 2, 3, 4, 5, and 6, we get the optimizing $\delta_m \approx 9.43$ for $\lambda = 2048$ and $\delta_m \approx 9.15$ for $\lambda = 3072$ respectively. In practice, δ for implementation must be an integer. Therefore, we can get the practical integer δ with the following corollary.

Corollary 2. *Let δ_m be a real number, and let $\mathcal{G}(\tau, \delta)$ denote a function in τ and δ . Define $\Delta = \delta_m - \lfloor \delta_m \rfloor$ as the fractional part of δ_m . Then, the relationship between $\mathcal{G}(\tau, \lfloor \delta_m \rfloor)$ and $\mathcal{G}(\tau, \lceil \delta_m \rceil)$ depends on Δ as follows:*

1. *If $\Delta < -\log_2(\ln 2)$, then $\mathcal{G}(\tau, \lfloor \delta_m \rfloor) < \mathcal{G}(\tau, \lceil \delta_m \rceil)$.*
2. *If $\Delta = -\log_2(\ln 2)$, then $\mathcal{G}(\tau, \lfloor \delta_m \rfloor) = \mathcal{G}(\tau, \lceil \delta_m \rceil)$.*

3. If $\Delta > -\log_2(\ln 2)$, then $\mathcal{G}(\tau, \lfloor \delta_m \rfloor) > \mathcal{G}(\tau, \lceil \delta_m \rceil)$.

Proof. See Appendix C. □

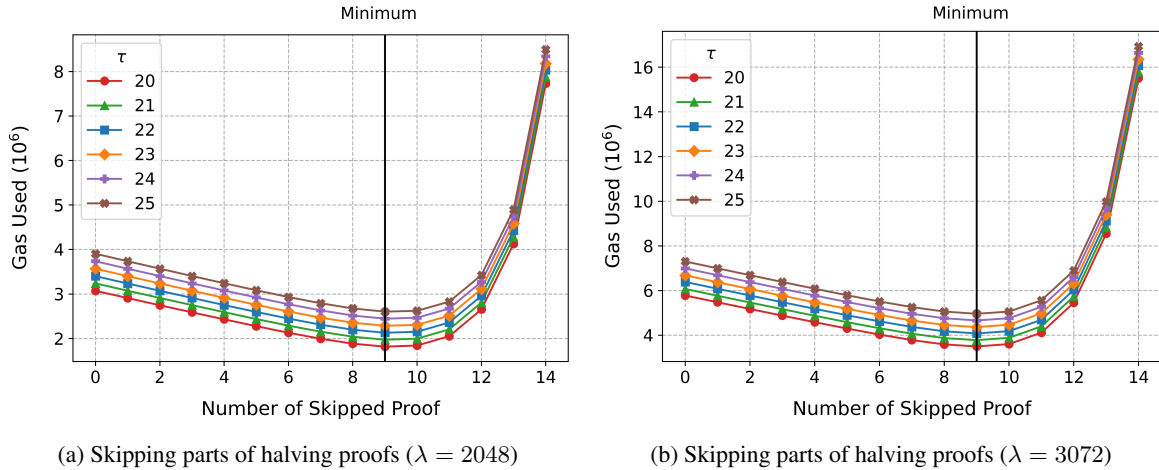
Since $\log_2(\ln 2) \approx -0.52$, the optimal integer value of δ is 9 for both $\lambda = 2048$ and 3072, as the 1st case of Corollary 2.

5.2 Optimized Verification Gas Cost

Figures 4a and 4b depict the total gas cost for Pietrzak VDF verification at $\lambda = 2048$ and $\lambda = 3072$ respectively. Consistent with the theoretical predictions in Theorem 1, the gas usage graph shows a decline to a minimal point before increasing sharply. Optimal gas costs were observed at $\delta = 9$ for both configurations, aligning perfectly with the findings of Corollary 2. This alignment between theoretical expectations and empirical results confirms the accuracy of our model and highlights its potential for optimizing Pietrzak VDF verification in blockchain applications.

Table 1 details the gas consumption and calldata sizes for the implemented parameters, uniformly using $\delta = 9$. Contrary to the previous expectation of calldata sizes around 40KB [7], the sizes recorded were significantly lower, ranging from 5.38 to 7.25 KB for $\lambda = 2048$ and from 7.13 to 9.63 KB for $\lambda = 3072$. Gas usage varied from 1.97 to 2.80 million for $\lambda = 2048$ and from 3.68 to 5.25 million for $\lambda = 3072$ ³. These findings not only demonstrate the efficacy of our approach but also highlight potential areas for further optimization in VDF implementations. Such improvements could lead to significant cost reductions in blockchain networks, enhancing the overall efficiency of cryptographic operations.

Figure 4: Results for halving proof skipping parameter δ with $\tau = 20, 21, 22, 23, 24, 25$ for $y = x^{2^{2^\tau}}$



6 Conclusion and Future Works

Our study demonstrates that Pietrzak’s VDF can be effectively optimized for the EVM, reducing gas costs from 4M to 2M and minimizing proof size to under 8 KB with a 2048-bit RSA key. These optimizations validate the theoretical models and show practical viability. While our paper does not address the Wesolowski VDF implementation, which poses challenges due to its hash-to-prime function, exploring indirect or approximate implementation methods could make it feasible for the EVM. Future work should focus on utilizing Wesolowski VDF verification on EVM as it has a big benefit on the constant and short proof length and verification cost. We plan to implement on-chain Wesolowski VDF verification both directly and indirectly. For indirect implementation, a hash-to-prime function could be executed in a Truebit-style proof-of-fraud system. For direct implementation, refining the hash-to-prime function to be viable and secure on the EVM is essential.

³Assuming 1 ETH is valued at \$2600, the cost for $\lambda = 2048$ ranges from approximately \$33.9 to \$136.6 USD when $\tau = 25$ and gasPrice varies between 5 and 20 gwei.

Table 1: Implementation results based on the analysis

λ	δ	τ	Gas used	Calldata size (KB)
2048	9	20	1817855	5.38
		21	1973222	5.75
		22	2129116	6.13
		23	2286058	6.50
		24	2445803	6.88
		25	2603753	7.25
3072	9	20	3495396	7.13
		21	3776893	7.63
		22	4078468	8.13
		23	4362630	8.63
		24	4658937	9.13
		25	4958138	9.63

References

- [1] B. Wesolowski, “Efficient verifiable delay functions,” in *Advances in Cryptology—EUROCRYPT 2019: 38th Annual International Conference on the Theory and Applications of Cryptographic Techniques, Darmstadt, Germany, May 19–23, 2019, Proceedings, Part III* 38, pp. 379–407, Springer, 2019.
- [2] K. Pietrzak, “Simple verifiable delay functions,” in *10th innovations in theoretical computer science conference (itsc 2019)*, Schloss-Dagstuhl-Leibniz Zentrum für Informatik, 2019.
- [3] A. K. Lenstra and B. Wesolowski, “Trustworthy public randomness with sloth, unicorn, and trx,” *International Journal of Applied Cryptography*, vol. 3, no. 4, pp. 330–343, 2017.
- [4] D. Khovratovich, M. Maller, and P. R. Tiwari, “Minroot: Candidate sequential function for ethereum vdf,” *Cryptology ePrint Archive*, 2022.
- [5] A. Biryukov, B. Fisch, G. Herold, D. Khovratovich, G. Leurent, M. Naya-Plasencia, and B. Wesolowski, “Cryptanalysis of algebraic verifiable delay functions,” *Cryptology ePrint Archive*, 2024.
- [6] G. Leurent, B. Mennink, K. Pietrzak, V. Rijmen, A. Biryukov, B. Bunz, A. Canteaut, I. Dinur, Y. Dodis, O. Dunkelman, *et al.*, “Analysis of minroot,” 2023.
- [7] V. Attias, L. Vigneri, and V. Dimitrov, “Implementation study of two verifiable delay functions,” *Cryptology ePrint Archive*, 2020.
- [8] R. L. Rivest, A. Shamir, and D. A. Wagner, “Time-lock puzzles and timed-release crypto,” 1996.
- [9] M. Mahmoody, T. Moran, and S. Vadhan, “Publicly verifiable proofs of sequential work,” in *Proceedings of the 4th conference on Innovations in Theoretical Computer Science*, pp. 373–388, 2013.
- [10] D. Boneh, J. Bonneau, B. Bünz, and B. Fisch, “Verifiable delay functions,” in *Annual international cryptology conference*, pp. 757–788, Springer, 2018.
- [11] K. Choi, A. Arun, N. Tyagi, and J. Bonneau, “Bicorn: An optimistically efficient distributed randomness beacon,” in *Financial Cryptography and Data Security: 27th International Conference, FC 2023, Bol, Brač, Croatia, May 1–5, 2023, Revised Selected Papers, Part I*, (Berlin, Heidelberg), p. 235–251, Springer-Verlag, 2023.
- [12] firo, “Full bignumber library implementation for solidity.” <https://github.com/firoorg/solidity-BigNumber>, 2024. Accessed: 2024-05-10.
- [13] A. Akhunov, E. Ben Sasson, T. Brand, L. Guthmann, and A. Levy, “Eip-2028: Transaction data gas cost reduction.” Ethereum Improvement Proposals, 2019. Accessed: 2024-05-10.
- [14] V. Buterin, “Eip-198: Big integer modular exponentiation.” Ethereum Improvement Proposals, 2017. Accessed: 2024-05-10.

- [15] K. Olson, S. Gulley, S. Peffers, J. Drake, and D. Feist, “Eip-2565: Modexp gas cost.” Ethereum Improvement Proposals, 2020. Accessed: 2024-05-10.

A Code availability

To facilitate reproducibility and peer review, we have made the source code for our implementation available anonymously. The repository contains all the scripts and supplementary materials necessary to reproduce the results discussed in this paper. You can access the repository at the following link: <https://github.com/usgeeus/Pietrzak-VDF-solidity-verifier>

B Proof of Theorem 1

Proof. Firstly, we calculate the partial derivative of \mathcal{G}_{total} with respect to δ , which yields

$$\frac{\partial \mathcal{G}_{total}}{\partial \delta} = \ln 2 \cdot \gamma \cdot 2^\delta - (\alpha + \beta).$$

To show that there is a unique δ that minimizes \mathcal{G}_{total} , we need to find where this derivative equals zero. This leads us to the equation

$$2^\delta = \frac{\alpha + \beta}{\ln 2 \cdot \gamma}.$$

The function 2^δ is strictly increasing. Hence, the equation $2^\delta = \frac{\alpha + \beta}{\ln 2 \cdot \gamma}$ has a unique solution δ , which can be expressed as

$$\delta = \log_2(\alpha + \beta) - \log_2(\ln 2 \cdot \gamma).$$

This δ is where the first derivative equals zero.

Further, to confirm that this δ is indeed a minimum, we need to check the second derivative. The monotonic nature of the exponential function in this context implies that as δ increases, $\gamma \cdot 2^\delta$ grows without bounds, while decreasing δ below this point leads to $\gamma \cdot 2^\delta$ becoming smaller than $\alpha + \beta$, thereby confirming that the function is minimized at this δ .

Thus, $\mathcal{G}_{total}(\tau, \delta)$ indeed has one unique minimum at δ within the specified range of $\tau > \delta \geq 0$, completing the proof. \square

C Proof of Corollary 2

Proof. Define

$$f(\delta) = \mathcal{G}(\tau, \delta + 1) - \mathcal{G}(\tau, \delta) = \gamma \cdot (2^{\delta+1} - 2^\delta) + (\alpha + \beta)(-(\delta + 1) + \delta) = \gamma \cdot 2^\delta - (\alpha + \beta). \quad (11)$$

Then, $f(\delta) = 0$ when

$$\delta = \log_2(\alpha + \beta) - \log_2 \gamma. \quad (12)$$

Also, as given $\gamma > 0, \delta > 0$

$$\frac{df}{d\delta} = \ln 2 \cdot \gamma \cdot 2^\delta, \quad (13)$$

f is a monotone-increasing function in the boundary. Therefore, after the point δ' where

$$\delta' = \log_2(\alpha + \beta) - \log_2 \gamma = \delta_m + \log_2(\ln 2), \quad (14)$$

f is bigger than 0.

For the 1st case of the lemma, $\Delta < -\log_2(\ln 2)$ implies

$$f(\lfloor \delta_m \rfloor) > 0. \quad (15)$$

As the definition of f ,

$$\mathcal{G}(\tau, \lfloor \delta_m \rfloor) < \mathcal{G}(\tau, \lceil \delta_m \rceil). \quad (16)$$

In the same way, we can get the other two cases. \square